Hindawi
Shock and Vibration
Volume 2021, Article ID 6643166, 10 pages
https://doi.org/10.1155/2021/6643166

Research Article

Optimization of Measuring Points Layout around a Tunnel in the Transversely Isotropic Rock Mass

Zhizeng Zhang,[1] **Yongtao Li**,[2] **Weili Yang**,[1] **Shunchuan Wu**,[3] **Xiaoli Liu**,[4] **and Bing Zhang**[5]

[1]*College of Civil Engineering and Architecture, Zhongyuan University of Technology, Zhengzhou 450007, China*
[2]*Department of Civil Engineering and Architecture, Zhengzhou Shengda University of Economics Business & Management, Zhengzhou 450007, China*
[3]*Kunming University of Science and Technology, Kunming 650093, China*
[4]*Department of Hydraulic and Hydropower Engineering, Tsinghua University, Beijing 100084, China*
[5]*R & D Department, State Key Laboratory of Shield Machine and Boring Technology, Zhengzhou 450001, China*

Correspondence should be addressed to Zhizeng Zhang; zhangzhizeng@163.com

Received 21 October 2020; Revised 6 January 2021; Accepted 16 January 2021; Published 27 January 2021

Academic Editor: Junfei Zhang

The arrangement of measuring points has a great impact on the uniqueness and accuracy of the back analysis of displacement. To explore the arrangement method of measuring points in the anisotropic rock mass, the principle of maximum displacement is applied to study the optimization of measuring points layout around a tunnel in the transversely isotropic rock mass. Firstly, the criterion of maximum displacement is deduced. Secondly, the variations of displacement with angle and radius are analyzed, respectively, and two key lateral pressure coefficients are obtained. Thirdly, some principles of measuring points arrangement are summarized according to the criterion of maximum displacement. Finally, an example is given to prove the correctness of these principles. These principles can be used to guide the arrangement of displacement measuring points in the transversely isotropic rock mass, especially suitable for shaft excavation in horizontal sedimentary rock.

1. Introduction

The arrangement of measuring points has a great impact on the uniqueness and accuracy of the back analysis of displacement [1]. Therefore, many researchers have studied the optimal arrangement of displacement measuring points. Kernevez et al. [2] found that it is not that the bigger the number of measuring points the better; instead, it was found that the spatial location of the measuring points is more important. Cividini et al. [3] and Venclik [4] discussed the issue of the number of measuring points and demonstrated that the number, quality, and spatial location of the measuring points should be considered comprehensively. Sun et al. [5] studied that the effect of increasing the number of measuring points on the back analysis results was not significant. The measuring point arrangement is also affected by other factors, such as sensitivity and the size of the measurement value. Zhou et al. [6] studied the in situ monitoring of auxiliary tunnel in deep mine. However, there is no unified standard to guide the layout of measuring points.

Currently, there are three principles that have formed theoretical systems: the principle of maximum displacement [7], the principle of maximum sensitivity [8], and the principle of minimum variance [9]. Xiang et al. [10, 11] proposed a criterion for optimizing the layout of measuring points considering the comprehensive influence of many factors and applied this criterion to the back analysis of material parameters in the field of geotechnical engineering and achieved good results. Su et al. [12] discussed the application of the least-square method in the displacement back analysis and used the three-dimensional finite element method in combination with the least-square method to

obtain parameters that are more in line with the actual engineering. The application of the optimized arrangement of measuring points in underground engineering has also been studied [13–17].

The rock mass was considered to be isotropic in the above studies. However, with the development of rock mechanics theory and experimental research, it is gradually recognized that anisotropy is an important property of rock mass. However, the measuring points layout around a tunnel in the anisotropic rock mass was rarely studied.

Based on the criterion of maximum displacement, this paper attempts to make a preliminary study on the optimal arrangement of measuring points in the back analysis of transversely isotropic rock masses and find some principles of displacement measuring points arrangement. Transversely isotropic rock masses mean that the rock mass has the same material constants in any direction parallel to the layer, while the material parameters in the vertical layers are different.

2. The Criterion of Maximum Displacement

Any measurement has an error, and it exists in lots of scientific experiments. Therefore, the error is usually used to characterize the accuracy of the measured data. There are four main sources of error. The first case is the device error, which is mainly caused by instrument accuracy. The second case is the environmental error, which is caused by the inconsistency of various environmental factors and the required standard status. The third case is human error, which is caused by the measurer himself. The fourth case is the method error, which is caused by the approximation of function types.

This article assumes that measurement errors only come from device errors. x^* is set to be the exact displacement of a measuring point and x is set to be the measured value. Therefore, $x^* - x$ is called the absolute error of x and $(x^* - x)/x^*$ is called the relative error. Because the exact value is often unknown in practice, $(x^* - x)/x$ is often used as the relative error of x.

If the reading accuracy of the instrument is δ, then the absolute error function satisfies

$$\left|x^* - x\right| \le \delta, \tag{1}$$

where δ is the absolute error bound of$x$ and $\delta/|x|$ is the relative error bound of x.

If there are multiple displacement measuring points around the tunnel, the average relative error bound can be expressed as

$$e = \frac{1}{n}\sum_{i=1}^{n}\frac{\delta}{\left|x_i\right|} = \frac{\delta}{n}\sum_{i=1}^{n}\frac{1}{\left|x_i\right|}, \tag{2}$$

where x_i is the measured value of the i-th measuring point; n is the total number of measuring points. The expression of e^* is set to

$$e^* = \frac{1}{n}\sum_{i=1}^{n}\frac{1}{\left|x_i\right|}. \tag{3}$$

Because δ is a fixed value, so the value of e can be directly evaluated by the value of e^*without having to consider the specific value of δ. If the measuring points are arranged in the area where the absolute value of the displacement is larger, then the smaller relative errors will be obtained.

Set the number of displacement measuring lines on the cross section of the tunnel as k, the number of measuring points on each line as l, and the displacement measurement value of each measuring point as u_{ij}. The formula of the average value of the relative error for the i-th measuring line can be written as

$$e_i = \frac{\delta}{n}\sum_{j=1}^{l}\frac{1}{\left|u_{ij}\right|}, \tag{4}$$

or

$$e_i^* = \frac{1}{n}\sum_{j=1}^{l}\frac{1}{\left|u_{ij}\right|}. \tag{5}$$

As can be seen from equation (5), the direction with the smallest e_i^* is the most suitable, and the magnitude of the relative error can be effectively reduced with the increased value of $|u_{ij}|$.

Based on the above analysis, the criterion for the optimal arrangement of displacement measuring points can be simply summarized as that the place with a larger absolute displacement value is more suitable to arrange measuring points.

3. Displacement Analytical Solution

Figure 1 presents an idealized model for a circular tunnel in the transversely isotropic rock mass.

Throughout this paper, the model with the following assumptions is used. The rock is continuous and linearly elastic, and the displacement and strain are tiny. The tunnel is deep. The cross section is circular and parallel to the transverse isotropic surface. The initial stress field in the rock mass is regarded as a normal stress p which acts in the vertical direction and a normal stress q which acts in the horizontal direction. The tunnel length is much bigger than its cross-sectional dimensions; thus, it can be simplified as a plane strain problem.

Zhang deduced the displacement analytical solution as follows [18]:

$$u_r = \frac{p+q}{2}\frac{a^2}{r}\frac{1+\mu}{E} + \frac{p-q}{2}\left[\frac{a^4}{r^3}\frac{1+\mu}{E} - \frac{4a^2}{r}\left(\frac{1}{E} - \frac{\mu'^2}{E'}\right)\right]\cos 2\theta, \tag{6}$$

where u_r is the radial displacement, E and μ are, respectively, the elastic modulus and Poisson's ratio in the isotropic plane, E' and μ' are corresponding elastic constants in the direction perpendicular to the isotropic plane, a is the radius of the tunnel, and r and θ are the polar diameter and angle in polar coordinates.

Introduce the side pressure coefficient $\lambda = q/p$ and equation (6) can be rewritten as

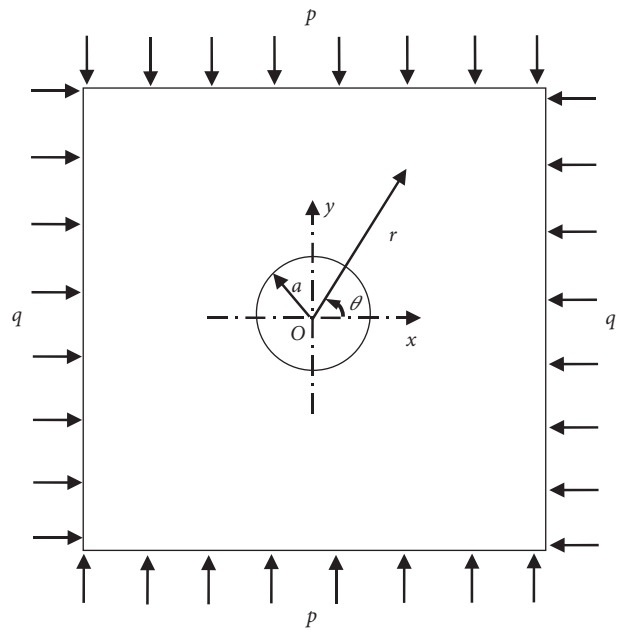

Figure 1: Model for a circular tunnel in transverse isotropy.

$$u_r = \frac{p}{2}(1+\lambda)\frac{a^2}{r}\frac{1+\mu}{E} + \frac{p}{2}(1+\lambda) \cdot \left[\frac{a^4}{r^3}\frac{1+\mu}{E} - \frac{4a^2}{r}\left(\frac{1}{E} - \frac{\mu'^2}{E'}\right)\right]\cos 2\theta, \tag{7}$$

where $u_r > 0$ means that the displacement direction points to the excavation surface and $u_r < 0$ means that the displacement direction is far from the excavation surface.

There exist the following restrictions between the parameters of transverse isotropy:

$$\frac{1}{E} < \frac{1+\mu}{E} < 2\left(\frac{1}{E} - \frac{\mu'^2}{E'}\right). \tag{8}$$

Since $a \le r$, it is easy to get

$$0 < \frac{a^4}{r^3} < \frac{2a^2}{r}. \tag{9}$$

Considering formulas (8) and (9) synthetically, the following formulas could be obtained:

$$\frac{a^4}{r^3}\frac{1+\mu}{E} - \frac{4a^2}{r}\left(\frac{1}{E} - \frac{\mu'^2}{E'}\right) < 0, \qquad \frac{p}{2}(1+\lambda)\frac{a^2}{r}\frac{1+\mu}{E} > 0. \tag{10}$$

These two formulas can be used to judge the monotonicity of the function in the following derivation.

4. Displacement Distribution Law of a Circular Tunnel in the Transversely Isotropic Rock Mass

4.1. Variation of Displacement with Angle. According to the value of λ, the distribution of displacement with angle is discussed in three cases.

(1) $\lambda = 1$

In this case, equation (7) becomes

$$u_r = \frac{p}{2}(1+\lambda)\frac{a^2}{r}\frac{1+\mu}{E}. \tag{11}$$

It can be seen that the displacement has nothing to do with θ, and the displacement is equal on a circle centered on the origin.

(2) $0 \le \lambda < 1$

In this case, u_r is a subtraction function of $\cos 2\theta$. In the area satisfying the relation $\cos 2\theta = -1$, u_r gets the maximum value.

$$u_{r\max} = \frac{p}{2}(1+\lambda)\frac{a^2}{r}\frac{1+\mu}{E} - \frac{p}{2}(1-\lambda) \cdot \left[\frac{a^4}{r^3}\frac{1+\mu}{E} - \frac{4a^2}{r}\left(\frac{1}{E} - \frac{\mu'^2}{E'}\right)\right]. \tag{12}$$

In the area satisfying the relation $\cos 2\theta = 1$, u_r gets the minimum value.

$$u_{r\min} = \frac{p}{2}(1+\lambda)\frac{a^2}{r}\frac{1+\mu}{E} + \frac{p}{2}(1-\lambda) \cdot \left[\frac{a^4}{r^3}\frac{1+\mu}{E} - \frac{4a^2}{r}\left(\frac{1}{E} - \frac{\mu'^2}{E'}\right)\right]. \tag{13}$$

(3) $\lambda > 1$

In this case, u_r is an increasing function of $\cos 2\theta$. In the area satisfying the relation $\cos 2\theta = 1$, u_r gets the maximum value.

$$u_{r\max} = \frac{p}{2}(1+\lambda)\frac{a^2}{r}\frac{1+\mu}{E} + \frac{p}{2}(1-\lambda) \cdot \left[\frac{a^4}{r^3}\frac{1+\mu}{E} - \frac{4a^2}{r}\left(\frac{1}{E} - \frac{\mu'^2}{E'}\right)\right]. \tag{14}$$

In the area satisfying the relation $\cos 2\theta = -1$, u_r gets the minimum value.

$$u_{r\min} = \frac{p}{2}(1+\lambda)\frac{a^2}{r}\frac{1+\mu}{E} - \frac{p}{2}(1-\lambda) \cdot \left[\frac{a^4}{r^3}\frac{1+\mu}{E} - \frac{4a^2}{r}\left(\frac{1}{E} - \frac{\mu'^2}{E'}\right)\right]. \tag{15}$$

Based on the above analysis, it can be seen that $u_{r\max}$ always appears in the direction of the larger initial ground stress, and $u_{r\min}$ always appears in the direction of the smaller initial ground stress.

Since $u_{r\max}$ is always positive and the relation $|u_{r\max}| \geq |u_{r\min}|$is always satisfied, the relation $|u_r|_{\max} = u_{r\max}$ can be obtained. However, $|u_r|_{\min}$ is not always equal to $u_{r\min}$, and the value of $|u_r|_{\min}$ is affected by the value of $u_{r\min}$. If $u_{r\min} \geq 0$, then $|u_r|_{\min} = u_{r\min}$. If $u_{r\min} < 0$, then $|u_r|_{\min} = 0$, and $|u_r|_{\min}$ appears in the area of $u_r = 0$, where $\cos 2\theta$ can be expressed as

$$\cos 2\theta = -\frac{(1+\lambda)((1+\mu)/E)}{(1-\lambda)\left[\left(a^2/r^2\right)((1+\mu)/E) - 4\left((1/E) - \left(\mu'^2/E'\right)\right)\right]}. \tag{16}$$

4.2. Variation of Displacement with Radius. Equation (7) can be rewritten as

$$u_r = \frac{p}{2}\frac{a^2}{r}\left[(1+\lambda)\frac{1+\mu}{E} - 4(1-\lambda)\left(\frac{1}{E} - \frac{\mu'^2}{E'}\right)\cos 2\theta\right] + \frac{p}{2}(1-\lambda)\frac{a^4}{r^3}\frac{1+\mu}{E}\cos 2\theta. \tag{17}$$

If $(1-\lambda)\cos 2\theta \neq 0$, then equation (17) can be rewritten as

$$u_r = \frac{p}{2}\frac{a^2}{r}\left[\frac{1+\lambda}{(1-\lambda)\cos 2\theta}\frac{1+\mu}{E} - 4\left(\frac{1}{E} - \frac{\mu'^2}{E'}\right) + \frac{a^2}{r^2}\frac{1+\mu}{E}\right](1-\lambda)\cos 2\theta. \tag{18}$$

Deviation of r yields

$$\frac{\mathrm{d}u_r}{\mathrm{d}r} = -\frac{p}{2}\frac{a^2}{r^2}\left[\frac{1+\lambda}{(1-\lambda)\cos 2\theta}\frac{1+\mu}{E} - 4\left(\frac{1}{E} - \frac{\mu'^2}{E'}\right) + \frac{3a^2}{r^2}\frac{1+\mu}{E}\right] \cdot (1-\lambda)\cos 2\theta. \tag{19}$$

Let equation (19) be equal to zero, so the extreme point can be obtained as follows:

$$r_e = \sqrt{\frac{3}{\left(4\left((1/E) - \left(\mu'^2/E'\right)\right)/(1+\mu/E)\right) - (1+\lambda/(1-\lambda)\cos 2\theta)a.}} \tag{20}$$

The following relation can be derived from formula (8):

$$2 < \frac{4\left((1/E) - \left(\mu'^2/E'\right)\right)}{(1+\mu/E)} < 4. \tag{21}$$

In addition, it is easy to prove the following formulas:

$$\left|\frac{1+\lambda}{1-\lambda}\right| \geq 1, \qquad \left|\frac{1+\lambda}{(1-\lambda)\cos 2\theta}\right| \geq 1. \tag{22}$$

According to the different combinations of parameters, the distribution of displacement with radius is discussed in two cases.

4.2.1. Case 1: $(1-\lambda)\cos 2\theta \leq (1+\lambda/4(1/E) - (\mu'^2/E') - (3/4)(1+\mu/E))(1+\mu/E)$. In this case, $|u_r|_{\max}$ always appears on the wall of the tunnel. There are four situations to discuss.

(1) $(1-\lambda)\cos 2\theta < 0$

It is easy to deduce

$$\frac{4\left((1/E) - \left(\mu'^2/E'\right)\right)}{(1+\mu/E)} - \frac{1+\lambda}{(1-\lambda)\cos 2\theta} > 3. \tag{23}$$

The relation $r_e < a$ can be obtained by substituting formula (23) into formula (20), and it is easy to judge that r_e is the maximum point according to formula (19). Because of $u_r|_{r=a} > 0$ and $u_r|_{r=\infty} = 0$, u_r monotonically decreases from $u_r|_{r=a}$ to 0 in the area where $r \geq a$. Correspondingly, $|u_r|_{\max}$appears on the tunnel wall, where $r = a$, and $|u_r|_{\min}$ appears at infinity.

(2) $(1-\lambda)\cos 2\theta = 0$

Equation (16) can be simplified as

$$u_r = \frac{p}{2}\frac{a^2}{r}(1+\lambda)\frac{1+\mu}{E}. \tag{24}$$

This case has the same conclusion as the case of $(1-\lambda)\cos 2\theta < 0$.

(3) $(1+\lambda/4((1/E) - (\mu'^2/E')))(1+\mu/E) \geq (1-\lambda)\cos 2\theta > 0$

The following formula can be derived:

$$\frac{4\left((1/E) - \left(\mu'^2/E'\right)\right)}{(1+\mu/E)} - \frac{1+\lambda}{(1-\lambda)\cos 2\theta} \leq 0. \tag{25}$$

In this case, formula (20) is meaningless, which shows that there are no local extreme points. Substituting formula (25) into formula (19) yields

$du_r/dr < 0$. This case has the same conclusion as that of the case of $(1-\lambda)\cos 2\theta < 0$.

(4) $(1+\lambda/4((1/E)-(\mu'^2/E'))-(3/4)(1+\mu/E))(1+\mu/E) \geq (1-\lambda)\cos 2\theta > (1+\lambda/4((1/E)-(\mu'^2/E')))(1+\mu/E)$

The following formula can be derived:

$$\frac{3}{4} \geq \frac{4\left((1/E)-\left(\mu'^2/E'\right)\right)}{(1+\mu/E)} - \frac{1+\lambda}{(1-\lambda)\cos 2\theta} > 0. \tag{26}$$

The relation $r_e > a$ can be obtained by substituting formula (26) into formula (20) and it is easy to judge that r_e is the minimum point according to formula (19). According to formula (18), there are

$$u_r|_{r=a} = \frac{p}{2}a\left[\frac{1+\lambda}{(1-\lambda)\cos 2\theta}\frac{1+\mu}{E} - 4\left(\frac{1}{E}-\frac{\mu'^2}{E'}\right)+\frac{1+\mu}{E}\right] \cdot (1-\lambda)\cos 2\theta > 0,$$

$$u_r|_{r=r_e} = -\frac{\sqrt{3}}{9}pa\left[4\left(\frac{1}{E}-\frac{\mu'^2}{E'}\right)-\frac{1+\lambda}{(1-\lambda)\cos 2\theta}\frac{1+\mu}{E}\right]^{3/2} \cdot \left(\frac{1+\mu}{E}\right)^{-(1/2)}(1-\lambda)\cos 2\theta < 0, \tag{27}$$

and $u_r|_{r=\infty} = 0$. In the area of $r \geq a$, u_r monotonically decreases from $u_r|_{r=a}$ to $u_r|_{r=r_e}$ and then monotonically increases to 0. Because of $|u_r|_{r=r_e}/u_r|_{r=a}| \leq 1$, $|u_r|_{\max}$ appears on the tunnel wall. $|u_r|_{\min}$ appears not only at infinity but also in the area indicated by the following equation:

$$r = \frac{a}{\sqrt{\left(4\left((1/E)-\left(\mu'^2/E'\right)\right)/(1+\mu/E)\right)-(1+\lambda/(1-\lambda)\cos 2\theta).}} \tag{28}$$

4.2.2. Case 2: $(1-\lambda)\cos 2\theta > (1+\lambda/4((1/E)-(\mu'^2/E'))-(3/4)(1+\mu/E))(1+\mu/E)$. In this case, $|u_r|_{\max}$ always appears at r_e. There are two situations to discuss.

(1) $(1+\lambda/4((1/E)-(\nu'^2/E'))-(1+\nu/E))(1+\nu/E) > (1-\lambda)\cos 2\theta > (1+\lambda/(4(1/E)-(\nu'^2/E'))-(3/4)(1+\nu/E))(1+\nu/E)$

The following formula can be deduced:

$$1 > \frac{4\left((1/E)-\left(\mu'^2/E'\right)\right)}{(1+\mu/E)} - \frac{1+\lambda}{(1-\lambda)\cos 2\theta} > \frac{3}{4}. \tag{29}$$

The relation $r_e > a$ can be obtained by substituting formula (29) into formula (20), and it is easy to judge that r_e is the minimum point according to formula (19). Because of $u_r|_{r=\infty} = 0$, u_r monotonically decreases to $u_r|_{r=r_e}$ and then monotonically increases to 0 in the area where $r \geq a$. Due to $|u_r|_{r=r_e}/u_r|_{r=a}| > 1$, $|u_r|_{\max}$ appears at r_e. $|u_r|_{\min}$ appears not only at infinity but also in the area indicated by equation (28).

(2) $(1-\lambda)\cos 2\theta \geq (1+\lambda/4((1/E)-(\nu'^2/E'))-(1+\mu/E))(1+\mu/E)$

The following formula can be deduced:

$$3 > \frac{4\left((1/E)-\left(\mu'^2/E'\right)\right)}{(1+\mu/E)} - \frac{1+\lambda}{(1-\lambda)\cos 2\theta} \geq 1. \tag{30}$$

The equation $r_e > a$ can be obtained by substituting formula (30) into formula (20), and it is easy to judge that r_e is the minimum point according to formula (19). According to formula (18), there are

$$u_r|_{r=a} = \frac{p}{2}a\left[\frac{1+\lambda}{(1-\lambda)\cos 2\theta}\frac{1+\mu}{E} - 4\left(\frac{1}{E}-\frac{\mu'^2}{E'}\right)+\frac{1+\mu}{E}\right] \cdot (1-\lambda)\cos 2\theta \leq 0,$$

$$u_r|_{r=r_e} = -\frac{\sqrt{3}}{9}pa\left[4\left(\frac{1}{E}-\frac{\mu'^2}{E'}\right)-\frac{1+\lambda}{(1-\lambda)\cos 2\theta}\frac{1+\mu}{E}\right]^{3/2} \cdot \left(\frac{1+\mu}{E}\right)^{-(1/2)}(1-\lambda)\cos 2\theta < 0. \tag{31}$$

Because of $u_r|_{r=\infty} = 0$, u_r monotonically decreases to $u_r|_{r=a}$ and then monotonically increases to 0 in the area of $r \geq a$. Correspondingly, $|u_r|_{\max}$ appears at r_e, and $|u_r|_{\min}$ appears at infinity.

4.2.3. The Influence of Lateral Pressure Coefficient on the Variation of Displacement with Radius. According to the above analysis, it is obvious that the variation of the displacement with radius caused by different combinations of parameters is different. The effect of the lateral pressure coefficient λ on the variation of displacement with radius is further analyzed below.

We have the following formula:

$$(1-\lambda)\cos 2\theta = \frac{1+\lambda}{4(1/E)-\left(\mu'^2/E'\right)-(3/4)(1+\mu/E)}\frac{1+\mu}{E}. \tag{32}$$

Then, there is

$$\cos 2\theta = \frac{(1+\lambda)(1+\mu/E)}{\left[4(1/E)-\left(\mu'^2/E'\right)-(3/4)(1+\mu/E\right)](1-\lambda)}. \tag{33}$$

Let equation (33) be equal to –1 and 1, respectively; λ_1 and λ_2 can be obtained:

$$\lambda_1 = \frac{4\left((1/E) - \left(\mu'^2/E'\right)\right) + (1/4)(1+\mu/E)}{4\left((1/E) - \left(\mu'^2/E'\right)\right) - (7/4)(1+\mu/E)}, \tag{34}$$

$$\lambda_2 = \frac{4\left((1/E) - \left(\mu'^2/E'\right)\right) - (7/4)(1+\mu/E)}{4\left((1/E) - \left(\mu'^2/E'\right)\right) + (1/4)(1+\mu/E)}. \tag{35}$$

It is easy to acquire the following two relations: $\lambda_1 > 1 > \lambda_2 > 0$ and $\lambda_1\lambda_2 = 1$. Here, λ_1 and λ_2 are referred to as the critical pressure coefficients of displacement. The discussion is divided into three cases.

(1) When $\lambda_1 \geq \lambda \geq \lambda_2$, all surrounding rock areas meet the conditions of formula (36), which is in full compliance with Section 4.2.1. So, the value of $|u_r|_{\max}$ is on the tunnel wall in all surrounding rock areas.

$$(1-\lambda)\cos 2\theta \leq \frac{1+\lambda}{4(1/E) - \left(\mu'^2/E'\right) - (3/4)(1+\mu/E)} \frac{1+\mu}{E}. \tag{36}$$

(2) When $\lambda > \lambda_1$, in the area indicated by formula (37), it is easy to deduce formula (38), which conforms to Section 4.2.1. So, the value of $|u_r|_{\max}$ is on the tunnel wall. In addition, this area decreases with the increase of λ.

$$\frac{(1+\mu/E)}{4(1/E) - \left(\mu'^2/E'\right) - (3/4)(1+\mu/E)} \frac{1+\lambda}{1-\lambda} \leq \cos 2\theta \leq 1, \tag{37}$$

$$(1-\lambda)\cos 2\theta \leq \frac{1+\lambda}{4(1/E) - \left(\mu'^2/E'\right) - (3/4)(1+\mu/E)} \frac{1+\mu}{E}. \tag{38}$$

However, in the area indicated by formula (39), it is easy to deduce formula (40), which conforms to Section 4.2.2. So, the value of $|u_r|_{\max}$ is at r_e. In addition, this area increases with the increase of λ.

$$-1 \leq \cos 2\theta < \frac{(1+\mu/E)}{4(1/E) - \left(\mu'^2/E'\right) - (3/4)(1+\mu/E)} \frac{1+\lambda}{1-\lambda}, \tag{39}$$

$$(1-\lambda)\cos 2\theta > \frac{1+\lambda}{4(1/E) - \left(\mu'^2/E'\right) - (3/4)(1+\mu/E)} \frac{1+\mu}{E}. \tag{40}$$

(3) When $0 \leq \lambda < \lambda_2$, in the area indicated by formula (41), it is easy to deduce formula (42), which accords with Section 4.2.1. So, the value of $|u_r|_{\max}$ is on the tunnel wall. In addition, this area increases with the increase of λ.

$$-1 \leq \cos 2\theta \leq \frac{(1+\mu/E)}{4(1/E) - \left(\mu'^2/E'\right) - (3/4)(1+\mu/E)} \frac{1+\lambda}{1-\lambda}, \tag{41}$$

$$(1-\lambda)\cos 2\theta \leq \frac{1+\lambda}{4(1/E) - \left(\mu'^2/E'\right) - (3/4)(1+\mu/E)} \frac{1+\mu}{E}. \tag{42}$$

However, in the area indicated by formula (43), it is easy to deduce formula (44), which accords with Section 4.2.2. So, the value of $|u_r|_{\max}$is at r_e. In addition, this area decreases with the increase of λ.

$$\frac{(1+\mu/E)}{4(1/E) - \left(\mu'^2/E'\right) - (3/4)(1+\mu/E)} \frac{1+\lambda}{1-\lambda} < \cos 2\theta \leq 1, \tag{43}$$

$$(1-\lambda)\cos 2\theta > \frac{1+\lambda}{4(1/E) - \left(\mu'^2/E'\right) - (3/4)(1+\mu/E)} \frac{1+\mu}{E}. \tag{44}$$

Based on the above analysis, it is known that $|u_r|_{\max}$ does not always appear on the tunnel wall; it may also appear at r_e under certain conditions.

5. The Principles of Measuring Points Arrangement for a Circular Tunnel in the Transversely Isotropic Rock Mass

According to the law of displacement distribution analyzed in Section 4, some principles of measuring point arrangement for a circular tunnel in the transversely isotropic rock mass can be obtained.

(1) The optimal direction of the displacement measuring line is the direction of the larger initial ground stress.

(2) If the displacement of the measuring points in the direction of the smaller initial ground stress is greater than or equal to zero, then this direction is the least suitable for measuring line layout. Conversely, if the displacement in the direction of the smaller initial ground stress is smaller than zero, the least suitable measuring line can be given by equation (16).

(3) When $\lambda_1 \geq \lambda \geq \lambda_2$, the most suitable measuring points are on the tunnel wall. When $\lambda > \lambda_1$or $0 \leq \lambda < \lambda_2$, in one part of the areas, the most suitable measuring points are on the tunnel wall, while in the other part of the areas, the most suitable measuring points are at r_e.

Figure 2 shows the flow chart for determining the optimal measuring line and measuring points.

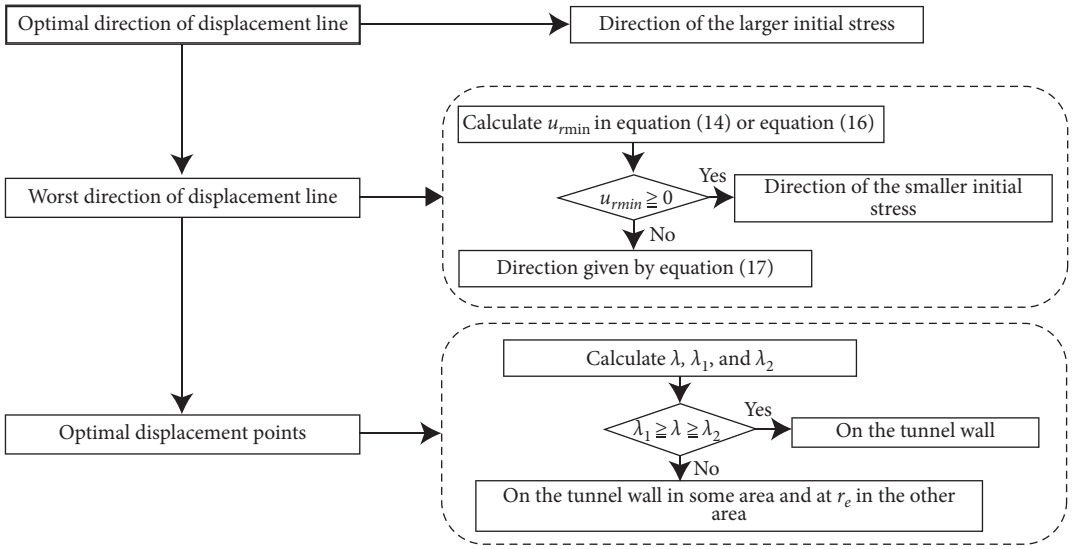

Figure 2: Flow chart for determining the optimal measuring line and measuring points.

In the displacement back analysis, if the initial ground stress is known, the measuring points can be arranged according to the research results in this section. If the ground stress is unknown, some additional measuring points can be arranged on a certain section of the tunnel firstly, and the initial ground stress can be identified based on the displacement of these measuring points.

6. Example of Measuring Points Layout

The parameters of a circular tunnel are, respectively, $a = 2$ m, $p = 10$ MPa, $E = 1$ GPa, $E' = 0.8$ GPa, $\mu = 0.25$, and $\mu' = 0.3$.

Due to the symmetry, only 1/4 of the surrounding rock area is used to study the measuring points layout, as shown in Figure 3. Seven radial displacement measuring lines are arranged on the measurement cross section. The angle between each measuring line is 15 degrees, and each line is 9 m in length. There are ten evenly arranged measuring points with a spacing of 1 m on each line, and each measuring point is numbered 1 ~ 10 according to the direction away from the tunnel wall.

By substituting the relevant parameters of this circular tunnel into equations (34) and (35), the critical pressure coefficients of displacement are obtained as $\lambda_1 = 2.83$ and $\lambda_2 = 0.35$. The layout of measuring points is discussed when λ is equal to 0, 0.5, 1, and 5, respectively, as follows.

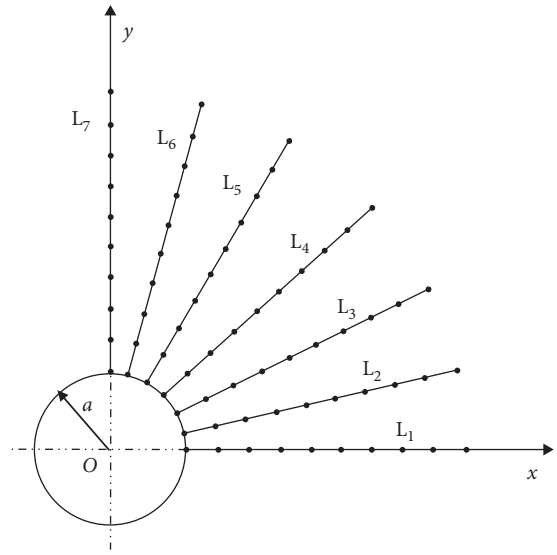

Figure 3: Measuring lines and points layout of a circular tunnel.

6.1. $\lambda = 0$. $\lambda = 0$ represents the situation of $0 \leq \lambda < \lambda_2$. The radial displacement of each measuring point is calculated according to equation (7), and then the average relative error of each measuring line is calculated according to equation (5). The results are listed in Table 1.

The following conclusions can be obtained from Table 1:

(1) The displacement increases as the angle increases from 0° to 90° for the measuring points with the same depth on different measuring lines. The measuring point with the maximum displacement (also the maximum displacement absolute value) appears in the L7 line, which is parallel to the larger initial ground stress. The measuring point with the minimum displacement always appears in the L1 line, which is parallel to the smaller initial ground stress. The measuring point with the minimum displacement absolute value appears in the L3 line. These verify the variation of displacement with an angle when $0 \leq \lambda < 1$ in Section 4.1.

(2) In the L4, L5, L6, and L7 lines, the measuring points with the maximum displacement absolute value appear on the cave wall, while in the L1, L2, and L3 lines, they do not appear on the cave wall. According to the deduction in Section 4.2, when $-1 \leq \cos 2\theta \leq 0.4784$ (corresponding to $30.71° \leq \theta \leq 90°$), the measuring point with the maximum displacement

Table 1: The radial displacements and average relative errors when $\lambda = 0$.

Line	Radial displacement of each measuring point										e_i^* (cm^{-1})
	N1 (cm)	N2 (cm)	N3 (cm)	N4 (cm)	N5 (cm)	N6 (cm)	N7 (cm)	N8 (cm)	N9 (cm)	N10 (cm)	
L1	−1.05	−1.16	−0.99	−0.84	−0.72	−0.63	−0.56	−0.50	−0.45	−0.41	1.55
L2	−0.74	−0.90	−0.78	−0.66	−0.57	−0.50	−0.44	−0.39	−0.36	−0.33	1.97
L3	0.10	−0.16	−0.18	−0.17	−0.15	−0.14	−0.12	−0.11	−0.10	−0.09	7.96
L4	1.25	0.83	0.63	0.50	0.42	0.36	0.31	0.28	0.25	0.23	2.60
L5	2.40	1.83	1.43	1.17	0.99	0.85	0.75	0.67	0.60	0.55	1.10
L6	3.24	2.56	2.03	1.66	1.40	1.21	1.06	0.95	0.86	0.78	0.78
L7	3.55	2.83	2.24	1.84	1.55	1.34	1.18	1.05	0.95	0.87	0.70

absolute value is on the cave wall; when $0.4784 < \cos 2\theta \le 1$ (corresponding to $0^\circ \le \theta < 30.71^\circ$), the measuring point is at r_e. These verify the variation of displacement with radius when $0 \le \lambda < \lambda_2$ in Section 4.2.

(3) It can be seen from e_i^* that the order of the layout of each measuring line is L7 > L6 > L5 > L1 > L2 > L4 > L3. This is by the principles of measuring points arrangement for a circular tunnel in the transversely isotropic rock mass in Section 5.

6.2. $\lambda = 0.5$. $\lambda = 0.5$ represents the situation of $\lambda_1 \ge \lambda \ge \lambda_2$. The radial displacements and average relative errors are calculated and listed in Table 2.

The following conclusions can be obtained from Table 2:

(1) The displacement increases as the angle increases from 0° to 90° for the measuring points with the same depth on different measuring lines. The measuring point with the maximum displacement (also the maximum displacement absolute value) appears in the L7 line, which is parallel to the larger initial ground stress. The measuring point with the minimum displacement (also the minimum displacement absolute value) appears in the L1 line, which is parallel to the smaller initial ground stress. These verify the variation of displacement with an angle when $0 \le \lambda < 1$ in Section 4.1.

(2) The measuring points with the maximum displacement absolute value appear on the cave wall in all the measuring lines. This verifies the variation of displacement with radius when $\lambda_1 \ge \lambda \ge \lambda_2$ in Section 4.2.

(3) It can be seen from e_i^* that the order of the layout of each measuring line is L7 > L6 > L5 > L4 > L3 > L2 > L1. This is by the principles of measuring points arrangement for a circular tunnel in the transversely isotropic rock mass in Section 5.

6.3. $\lambda = 1$. $\lambda = 1$ corresponds to the axisymmetric problem, which is often encountered in engineering. $\lambda = 1$ represents the situation of $\lambda_1 \ge \lambda \ge \lambda_2$. The radial displacements and average relative errors are calculated and listed in Table 3.

The following conclusions can be obtained from Table 3:

(1) The displacements are all positive and do not vary with an angle for the measuring points with the same depth on different measuring lines. This verifies the variation of displacement with an angle when $\lambda = 1$ in Section 4.1.

(2) The measuring points with the maximum displacement absolute value appear on the cave wall in all the measuring lines. This verifies the variation of displacement with radius when $\lambda_1 \ge \lambda \ge \lambda_2$ in Section 4.2.

(3) As can be seen from e_i^*, the average relative errors of all measuring lines are equal, which demonstrates that there is no distinction between good and bad for different measuring lines.

6.4. $\lambda = 5$. $\lambda = 5$ represents the situation of $\lambda > \lambda_1$. The radial displacements and average relative errors are calculated and listed in Table 4.

The following conclusions can be obtained from Table 4:

(1) The displacement decreases as the angle increases from 0° to 90° for the measuring points with the same depth on different measuring lines. The measuring point with the maximum displacement (also the maximum displacement absolute value) appears in the L1 line, which is parallel to the larger initial ground stress. The measuring point with the minimum displacement appears in the L7 line, which is parallel to the smaller initial ground stress. The measuring point with the minimum displacement absolute value appears in the L5 or L6 line. These verify the variation of displacement with an angle when $\lambda > 1$ in Section 4.1.

(2) In the L1, L2, L3, L4, and L5 lines, the measuring points with the maximum displacement absolute value appear on the cave wall, while in the L6 and L7 lines, they do not appear on the cave wall. According to the deduction in Section 4.2, when $0.7177 < \cos 2\theta \le 1$ (corresponding to $0^\circ \le \theta < 67.93^\circ$), the measuring point with the maximum displacement absolute value is on the cave wall; when $-1 \le \cos 2\theta \le 0.7177$ (corresponding to $67.93^\circ \le \theta \le 90^\circ$), the measuring point is at r_e. These verify the variation of displacement with radius when $0 \le \lambda < \lambda_2$ in Section 4.2.

Table 2: The radial displacements and average relative errors when $\lambda = 0.5$.

Line	Radial displacement of each measuring point										e_i^* (cm^{-1})
	N1 (cm)	N2 (cm)	N3 (cm)	N4 (cm)	N5 (cm)	N6 (cm)	N7 (cm)	N8 (cm)	N9 (cm)	N10 (cm)	
L1	0.73	0.25	0.13	0.08	0.06	0.04	0.03	0.03	0.02	0.02	21.53
L2	0.88	0.39	0.24	0.17	0.13	0.11	0.09	0.08	0.07	0.06	8.30
L3	1.30	0.75	0.53	0.42	0.34	0.29	0.25	0.22	0.20	0.18	3.17
L4	1.88	1.25	0.94	0.75	0.63	0.54	0.47	0.42	0.38	0.34	1.73
L5	2.45	1.75	1.34	1.09	0.91	0.78	0.69	0.61	0.55	0.50	1.19
L6	2.87	2.11	1.64	1.33	1.12	0.96	0.84	0.75	0.68	0.62	0.97
L7	3.03	2.25	1.75	1.42	1.19	1.03	0.90	0.80	0.73	0.66	0.91

Table 3: The radial displacements and average relative errors when $\lambda = 1$.

Line	Radial displacement of each measuring point										e_i^* (cm^{-1})
	N1 (cm)	N2 (cm)	N3 (cm)	N4 (cm)	N5 (cm)	N6 (cm)	N7 (cm)	N8 (cm)	N9 (cm)	N10 (cm)	
L1	2.50	1.67	1.25	1.00	0.83	0.71	0.63	0.56	0.50	0.45	1.30
L2	2.50	1.67	1.25	1.00	0.83	0.71	0.63	0.56	0.50	0.45	1.30
L3	2.50	1.67	1.25	1.00	0.83	0.71	0.63	0.56	0.50	0.45	1.30
L4	2.50	1.67	1.25	1.00	0.83	0.71	0.63	0.56	0.50	0.45	1.30
L5	2.50	1.67	1.25	1.00	0.83	0.71	0.63	0.56	0.50	0.45	1.30
L6	2.50	1.67	1.25	1.00	0.83	0.71	0.63	0.56	0.50	0.45	1.30
L7	2.50	1.67	1.25	1.00	0.83	0.71	0.63	0.56	0.50	0.45	1.30

Table 4: The radial displacements and average relative errors when $\lambda = 5$.

Line	Radial displacement of each measuring point										e_i^* (cm^{-1})
	N1 (cm)	N2 (cm)	N3 (cm)	N4 (cm)	N5 (cm)	N6 (cm)	N7 (cm)	N8 (cm)	N9 (cm)	N10 (cm)	
L1	16.70	12.99	10.23	8.36	7.05	6.08	5.35	4.77	4.30	3.92	0.15
L2	15.47	11.92	9.36	7.64	6.44	5.56	4.88	4.35	3.92	3.57	0.17
L3	12.10	8.99	6.99	5.68	4.77	4.11	3.61	3.22	2.90	2.64	0.23
L4	7.50	5.00	3.75	3.00	2.50	2.14	1.88	1.67	1.50	1.36	0.43
L5	2.90	1.01	0.51	0.32	0.23	0.17	0.14	0.12	0.10	0.09	5.38
L6	−0.47	−1.92	−1.86	−1.64	−1.44	−1.27	−1.13	−1.02	−0.92	−0.85	0.94
L7	−1.70	−2.99	−2.73	−2.36	−2.05	−1.80	−1.60	−1.43	−1.30	−1.19	0.57

(3) It can be seen from e_i^* that the order of the layout of each measuring line is L1 > L2 > L3 > L4 > L7 > L6 > L5. This is by the principles of measuring points arrangement for a circular tunnel in the transversely isotropic rock mass in Section 5.

7. Conclusions

This paper studies the optimization of the location of measuring points layout around a circular tunnel in the transversely isotropic rock mass. Based on the principle of maximum displacement, the variation of displacement with angle and radius was analyzed in detail, some layout principles were obtained, and these principles were verified through an example. The main conclusions are as follows:

(1) The criterion for the optimal arrangement of displacement measuring points can be simply summarized as that the place with a larger absolute displacement value is more suitable to arrange measuring points.

(2) The two critical side pressure coefficients λ_1 and λ_2 suitable for a circular tunnel in the transversely isotropic rock mass are derived. When $\lambda_1 \geq \lambda \geq \lambda_2$, the most suitable measuring points are on the tunnel wall. When $\lambda > \lambda_1$ or $0 \leq \lambda < \lambda_2$, in one part of the areas, the most suitable measuring points are on the tunnel wall, while in the other part of the areas, the most suitable measuring points are at r_e.

(3) The optimal direction of the displacement measuring line is the direction of the larger initial ground stress.

(4) The area near the cave wall in the direction of the larger principal stress is the most suitable area to arrange measuring points.

Data Availability

The data used to support the findings of this study are available from the corresponding author upon request.

Conflicts of Interest

The authors declare no conflicts of interest.

Acknowledgments

This research was supported by the Special Funds of the National Natural Science Foundation of China (nos. 51934003, 51774020, and U1204509), Program for Yunnan Thousand Talents Plan High-level Innovation and Entrepreneurship Team, and Program for Innovative Research Team (in Science and Technology) at University of Yunnan Province.

References

[1] Z. Zhang, X. Li, and Y. Li, "Uniqueness of displacement back analysis of a deep tunnel with arbitrary cross section in transversely isotropic rock," *International Journal of Rock Mechanics and Mining Sciences*, vol. 97, pp. 110–121, 2017.

[2] J. P. Kernevez, C. Knopf-Lenoir, G. Touzot, and G. Verchery, "An identification method applied to an orthotropic plate bending experiment," *International Journal for Numerical Methods in Engineering*, vol. 12, no. 1, pp. 129–139, 1978.

[3] A. Cividini, L. Jurina, and G. Gioda, "Some aspects of "characterization" problems in geomechanics," *International Journal of Rock Mechanics and Mining Sciences & Geomechanics Abstracts*, vol. 18, no. 6, pp. 487–503, 1981.

[4] P. Venclik, "Development of an inverse back analysis code and its verification," in *Proceedings, European Conference on Numerical Methods in Geotechnical Engineering*, pp. 423–430, Porto, Portugal, June 1994.

[5] J. Sun, S. P. Jiang, and Y. Yuan, *Stochastic Theory and Method for Rock Mechanics Inversion*, Shantou University Press, Shantou, China, 1996.

[6] H. Zhou, C.-K. Qu, D.-W. Hu et al., "In situ monitoring of tunnel deformation evolutions from auxiliary tunnel in deep mine," *Engineering Geology*, vol. 221, pp. 10–15, 2017.

[7] L. D. Yang, M. Peng, and , and X. F. Ma, "Optimization of the displacement measuring in surrounding rock," *Journal of TongJi University*, vol. 23, no. 2, pp. 129–133, 1995.

[8] L. J. Wardle and C. M. Gerrard, "The "equivalent" anisotropic properties of layered rock and soil masses," *Rock Mechanics Felsmechanik Mécanique des Roches*, vol. 4, no. 3, pp. 155–175, 1972.

[9] M. M. Mejias, H. R. B. Orlande, and M. N. Özisik, "Effects of the heating process and body dimensions on the estimation of the thermal conductivity components of orthotropic solids," *Inverse Problems in Engineering*, vol. 11, no. 1, pp. 75–89, 2003.

[10] Z. H. Xiang, G. Svvubuda, and Z. Cen, "Parameter idenliualiun and its application in tunneling," in *Numerical Simulation in Tunneling*, G. Beer, Ed., pp. 161–200, Springer-Verlag, Berlin, Germany, 2003.

[11] Z. Xiang, G. Swoboda, and Z. Cen, "Optimal layout of displacement measurements for parameter identification process in geomechanics," *International Journal of Geomechanics*, vol. 3, no. 2, pp. 205–216, 2003.

[12] X. Z. Su, J. D. He, and Y. Luo, "Application of least squares method in back analysis of displacement," *Western Exploration Project*, vol. 1, pp. 145–147, 2007.

[13] Y. T. C. Jim and S. Liu, "Hydraulic tomography: development of a new aquifer test method," *Water Resources Research*, vol. 36, no. 8, pp. 2095–2105, 2000.

[14] J. Cunha and J. Piranda, "Application of model updating techniques in dynamics for the identification of elastic constants of composite materials," *Composites Part B: Engineering*, vol. 30, no. 1, pp. 79–85, 1999.

[15] K. T. Kavanagh, "Experiment versus analysis: computational techniques for the description of static material response," *International Journal for Numerical Methods in Engineering*, vol. 5, no. 4, pp. 503–515, 1973.

[16] J. Cunha and J. Piranda, "Identification of stiffness properties of composite tubes from dynamic tests," *Experimental Mechanics*, vol. 40, no. 2, pp. 211–218, 2000.

[17] R. T. Haftka, E. P. Scott, and J. R. Cruz, "Optimization and experiments: a survey," *Applied Mechanics Reviews*, vol. 51, no. 7, pp. 435–448, 1998.

[18] Z. Zhang and X. Li, "Displacement analytical solution of a circular hole in layered composite materials considering shear stress," *Advanced Composite Letters*, vol. 3, pp. 77–81, 2017.